ACS APPLIED MATERIALS & INTERFACES

Research Article

www.acsami.org

# Colloidal $CuInSe_2$ Nanocrystals: From Gradient Stoichiometry toward Homogeneous Alloyed Structure Mediated by Conducting Polymer P3HT

Yen Nan Liang,[†] Kui Yu,[‡] Qingyu Yan,[†] and Xiao Hu*,[†]

[†]School of Materials Science and Engineering, Nanyang Technological University, Nanyang Avenue, Singapore 639798

[‡]Steacie Institute for Molecular Sciences, National Research Council of Canada, Ottawa, Ontario, Canada

Supporting Information

**ABSTRACT:** We report, for the first time, the synthesis of colloidal copper indium selenide ($CuInSe_2$) nanocrystals (NCs) possessing a gradient stoichiometry that is potentially tunable by the presence of a conducting polymer, i.e., poly(3-hexyl thiophene) (P3HT) in the synthesis medium. Dibenzyl ether (DBE) was used as a reaction medium, whereas copper acetylacetonate ($Cu(acac)_2$), indium acetylacetonate ($In(acac)_3$), and selenium powder were used as Cu, In, and Se sources, respectively. The Se precursor was tri-n-octylphosphine selenide (TOP-Se). Without the presence of P3HT, the resulting NCs consist of a p-type ($Cu^{1+}$ rich) core and an n-type ($In^{3+}$ rich) shell. Such a gradient stoichiometry was moderated to be substantially more homogeneous because the presence of P3HT is believed to have significantly reduced the reactivity difference between $Cu(acac)_2$ and $In(acac)_3$, as well as and their respective monomers. Furthermore, the P3HT also acts as a surface coordination species, contributing to the readily preparation of conducting polymer-NCs hybrids by a single-step synthesis. The understandings of this work can serve as a guide for design and synthesis of conducting polymer-NCs hybrids based on various ternary or quaternary compound semiconductors with different core−shell composition gradient.

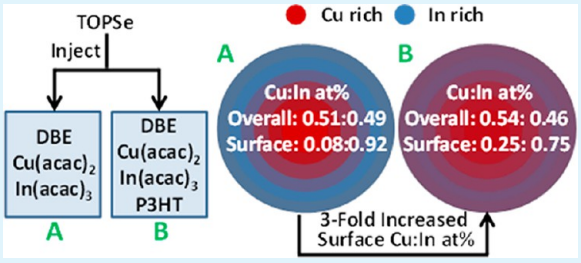


**KEYWORDS:** *$CuInSe_2$ nanocrystals, gradient stoichiometry, core−shell structure, precursor reactivity, poly(3-hexyl thiophene), polymer assisted synthesis*

## 1. INTRODUCTION

Conducting polymer−nanocrystals (NCs) hybrids,[1,2] consisting of nanoscale intermixed conducting polymer and functional inorganic NCs, represent a class of materials that can be directly incorporated into various functional devices by solution-phase process. The relevant devices, mainly photovoltaics, utilize the novel and synergistic optoelectronic properties of the hybrids, e.g., widened absorption wavelength range and quantum confinement effect.[3,4] Polymer−NC interface critically affects the device performance and is dependent on the coordination species on the NC surface.[5] The conventional blending of the presynthesized NCs with polymers tends to create non-optimum interface that hinders charge transfer and causes undesirable charge trapping or recombination. Therefore, an additional step of ligand exchange is almost always a must in order to remove the surface-bound ligand which was used during the synthesis of NC. To bypass the ligand issue, there have been attempts of directly synthesizing the NCs in the presence of conducting polymers. Some previously demonstrated examples include CdSe in P3HT,[6] CdS in P3HT,[3,7] in poly(2-methoxy-5-(2′-ethyl-hexyloxy)-*p*-phenylene)[8,9] or in polyphenylene-*b*-poly(2-vinyl pyridine),[10] and PbS in P3HT.[11,12] Intimate interface was evidenced through longer decay time of charge carrier[6] and photoluminescence quenching.[10] Synthesis of NCs in the presence of a conducting polymers offers advantages of simplicity and reducing the usage of insulating ligands. However, there is little discussion on the interaction between the conducting polymers with the NC precursors during synthesis and its implication on the structural formation. Besides, there is no report on using conducting polymers in the synthesis of ternary compound semiconductor NCs.

Copper indium selenide ($CuInSe_2$), a promising photovoltaic material,[13] can be prepared by a range of colloidal synthesis methods that are broadly categorized into (i) heating-up method,[14] (ii) autoclave solvothermal method,[15,16] and (iii) hot-injection method.[17−19] Colloidal $CuInSe_2$ NCs with different morphologies[20,21] and different crystal phases[22−24] were reported. $CuInSe_2$ NCs have recently been used in photovoltaics (fully inorganic[20,25−27] or hybrid[28,29]) and photoconductors[24,30,31] with limited success. In fact, the effect of inhomogeneous stoichiometry is well-appreciated in the studies of $CuInSe_2$ thin film.[13,32,33] The functional properties of $CuInSe_2$ and device performance are critically impacted by its

Received: December 23, 2012
Accepted: April 16, 2013
Published: April 16, 2013

  

Table 1. Synthesis Parameters Used for Different $CuInSe_2$ NCs Samples Prepared without or with P3HT

| set of conditions | $Cu(acac)_2$ (mg) | $In(acac)_3$ (mg) | Se (mg) | P3HT (mg) | DBE (ml) | TOP (ml) | Injection temp. (°C) | Growth temp. (°C) |
|---|---|---|---|---|---|---|---|---|
| A[a] | 87.7 | 138.1 | 216 | | 3.4 | 3.4 | 290 | 260 |
| B[a] | 87.7 | 138.1 | 216 | | 10 | 2 | 290 | 260 |
| C[a] | 87.7 | 138.1 | 216 | 5 | 10 | 2 | 290 | 260 |

[a]Condition A uses higher concentrations of precursor and ligand with reduced amount of solvent comparing with B. condition C is the same as B except that 5 mg of P3HT is used.

stoichiometry. The stoichiometry of solution synthesized $CuInSe_2$ NCs was found to be sensitive to parameters including types of precursor,[17,25,26] types of ligand,[23] and injection temperature.[18] However, previous studies mostly viewed the $CuInSe_2$ NCs to have overall uniform stoichiometry, with little discussion the inhomogeneous stoichiometry within one particle. Nevertheless, on the basis of the fact that there is a reactivity difference between the two metallic species precursors, it is not difficult to deduce an intrinsic tendency of inhomogeneous stoichiometry within a crystal. Therefore, a systematic study is needed to understand this aspect on the basis of crystal nucleation and growth. The kinetics of precursor conversion into binary monomers is crucial because the ternary chalcogenides, e.g., $CuInSe_2$, involve more than one metal source. Despite the ongoing controversy over the formation pathways, the critical influence of coordination species toward reaction kinetics was reported in several studies of binary chalcogenides (e.g., PbSe).[34−36] Therefore, it is anticipated that new and interesting phenomena will arise when ternary $CuInSe_2$ NCs are studied in this context especially when they are synthesized in the presence of a conducting polymer. This work reports for the first time a single-injection synthesis of hybrids containing P3HT coordinated $CuInSe_2$ NCs with novel core−shell-like stoichiometry, i.e., Cu-rich core and In-rich shell. Synthesis without P3HT led to highly gradient stoichiometry, while the presence of P3HT in the synthesis medium, besides improving the interfacial properties by coordinating to the NCs, significantly moderated the core−shell-like gradient stoichiometry within the NCs. Further discussion is carried out on the possible mechanisms that are responsible for the gradient stoichiometry and the role of P3HT in tuning the radial composition in the $CuInSe_2$ NCs.

## 2. EXPERIMENTAL SECTION

**2.1. Materials and Hot-Injection Synthesis.** Copper acetylacetonate ($Cu(acac)_2$), indium acetylacetonate ($In(acac)_3$), selenium powder (Se), tri-n-octylphosphine (TOP), dibenzyl ether (DBE), regioregular poly(3-hexyl thiophene) (P3HT), all from Sigma-Aldrich, were used in synthesis without further purification. $Cu(acac)_2$ and $In(acac)_3$ of 1:1 molar ratio were added to DBE in a three-neck flask, and this mixture is referred as the "precursor solution". P3HT, if included, was added and dissolved in the "precursor solution" in this step. TOP-Se was prepared in a separate flask by dissolving Se in TOP at 55 °C aided by stirring. TOP-Se preparation was done inside a glovebox under $N_2$ atmosphere. The "precursor solution" was then heated at 100 °C for 3 h and at 140 °C for 1 h to obtain a homogeneous reaction solution. After that, it was heated to 290 °C, and swift injection of TOP-Se was carried out. The temperature was then reduced to 260 °C for growth. The reaction was considered to have started after the injection and aliquots (e.g., 3 mL) were extracted at fixed time intervals for characterization. For purification, each aliquot was allowed to cool to room temperature before flocculation by adding ethanol and sonication for 20 min. It was then centrifuged at 4500 rpm to remove byproducts. Further purification was carried out by sonicating products in toluene/ethanol mixture (2:1 volume ratio) for 20 min, before centrifugation at 9000 rpm for 15 min. The supernatant portion was discarded and the solid content was redispersed in toluene/ethanol mixture aided by sonication. This process was repeated three times. After that, the NCs were dispersed in toluene and used for further characterization. Summarized in Table 1 are the synthesis parameters used under different conditions. Under each set of condition, NC samples were obtained at different reaction durations.

**2.2. Characterizations.** Thin film X-ray diffraction (TFXRD) was carried out using a Shimadzu X-ray diffractometer equipped with a Cu k$\alpha$ ($\lambda$ = 1.54 Å) X-ray source operated at 40 kV and 30 mA. Atomic absorption spectroscopy (AAS) was carried out using a Perkin-Elmer AAnalyst100 system. X-ray photoelectron spectroscopy (XPS) was carried out using AXIS HSI-165 Ultra, Kratos Analytical, equipped with Al K$\alpha$ X-ray source. Energy-dispersive X-ray spectroscopy (EDX) was carried out using a JEOL JSM 6360 scanning electron microscope (SEM) equipped with an EDX detector. Transmission electron microscopy (TEM) images were collected using a JEOL 2100 TEM. UV−vis NIR absorption spectra of dispersed NC samples in toluene were recorded using Shimadzu UV-3101PC spectrometer.

## 3. RESULTS

**3.1. Crystal Phase of $CuInSe_2$ Nanocrystals.** From the TFXRD spectra (Figure 1), it can be verified that all the synthesized nanocrystals (NCs) are of chalcopyrite phase (JCPDS# 40−1487), i.e., an alloyed phase instead of simply mixture of $Cu_{2-x}Se$ and $In_2Se_3$. The initial formation of binary intermediates (CuSe, $Cu_{2-x}Se$, and $In_2Se_3$) is expected, which then react to form chalcopyrite $CuInSe_2$. There is no observable effect of P3HT toward the crystal structures. The synthesized NCs are unlikely to be discrete particle aggregated from binary intermediates because no detectable $In_2Se_3$ phase was observed in XRD spectra. The only exception is the sample prepared under condition A-6 min which clearly shows the existence of CuSe intermediate. However, it should be mentioned that the prominent XRD peak positions of $Cu_{2-x}Se$ (JCPDS# 46−1129) are similar to those of $CuInSe_2$, and were not quantitatively distinguishable in XRD spectra obtained by the diffractometer.

**3.2. Stoichiometric Properties of $CuInSe_2$ Nanocrystals.** The novel gradient stoichiometry (Cu-rich core and In-rich shell) of the $CuInSe_2$ NCs could be deduced from combined analysis of AAS (overall stoichiometry) and XPS (surface stoichiometry) (see data in Table 2). Overall stoichiometry of all $CuInSe_2$ NCs, as shown by AAS results, is close to Cu:In = 1:1 (slightly Cu-rich). Interestingly, the surface stoichiometry as revealed by XPS shows exceptionally high In:Cu atomic ratio. EDX was also employed for stoichiometric determination, and the results show that $CuInSe_2$ NCs are In-rich. In fact, considering all three different types of stoichiometry results, the inadequacy of EDX technique is obvious due to its semi-quantitative nature and larger error margin. Therefore, EDX results should not be overly interpreted as they may lead to erroneous conclusion if not carefully analyzed.

The detailed binding energy (BE) spectra of Cu2p and In3d core levels are shown in Figure 2. The major BE peak positions of our XPS spectra are consistent with the theoretical $CuInSe_2$

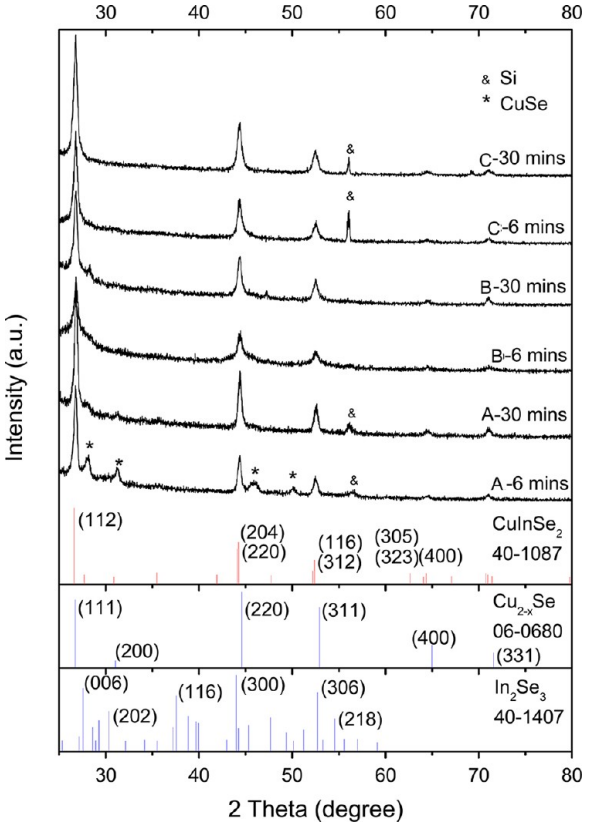


**Figure 1.** TFXRD spectra of synthesized $CuInSe_2$ NCs of 6 and 30 min synthesis durations using: (a) condition A; (b) condition B; and (c) condition C. The standard XRD patterns of $CuInSe_2$, $Cu_{2-x}Se$, and $In_2Se_3$ are included for reference.

**Table 2. Summary of Overall and Surface Atomic Percentage (at %) of Cu and In; as Obtained from AAS and XPS; EDX Results Are Also Included for Comparison**

| | | atomic % | | | |
|---|---|---|---|---|---|
| | | 6 min | | 30 min | |
| | set of conditions | Cu | In | Cu | In |
| overall (AAS) | A | 0.52 | 0.48 | 0.52 | 0.48 |
| | B | 0.57 | 0.43 | 0.51 | 0.49 |
| | C | 0.60 | 0.40 | 0.54 | 0.46 |
| surface (XPS)[a] | A | 0.00 | 1.00 | 0.03 | 0.97 |
| | B | 0.06 | 0.94 | 0.08 | 0.92 |
| | C | 0.14 | 0.86 | 0.25 | 0.75 |
| EDX | A | 0.38 | 0.62 | 0.38 | 0.62 |
| | B | 0.28 | 0.72 | 0.32 | 0.68 |
| | C | 0.38 | 0.62 | 0.32 | 0.67 |

[a]To obtain more accurate photoelectron signal, we removed the coordination species of XPS samples by following steps: (i) sonication inside ethanolic solution containing hydrazine, (ii) after sonication, the products were repeatedly washed with ethanol to remove remaining hydrazine.

BE peak positions, but all with slightly larger BE values (especially for Cu2p core level BE), which is associated with minor surface oxidation during sample preparation. Note that for all conditions A, B, and C, the BE values of samples synthesized at 30 min duration are closer to theoretical values than those obtained at 6 min, indicating the reactions are more complete at longer duration. Especially for the A-6 min sample, the Cu2p BE spectrum suggests zero Cu on the NCs surface; and its In3d BE spectrum shows a double BE peak, which may be an indication that the alloying reaction is incomplete giving rise to In with different valence states. The results also confirm that XPS is a more sensitive technique for composition analysis than XRD.

Despite the matched core level BE peak positions, the relative intensities of Cu2p and In3d BE peaks are distinctly different from an earlier reported $CuInSe_2$ XPS spectrum.[24] Samples prepared under condition B using lower precursor concentrations appear to have a less gradient stoichiometry (Table 2). With the presence of P3HT (condition C), a considerable moderation of gradient stoichiometry is observed, with a 3 time increase in surface Cu concentration than the sample prepared without P3HT (condition B) (see Table 2). Therefore, combining both AAS and XPS results, the $CuInSe_2$ NCs are shown to possess Cu-rich core and In-rich shell and the gradient stoichiometry can be substantially moderated by using a very small amount of P3HT.

**3.3. Morphological Properties of $CuInSe_2$ Nanocrystals.** Figure 3 shows that the morphology of NC samples synthesized is either near-spherical or irregular. This morphology is generally consistent with previous report that used acetylacetonate precursors.[17] The $CuInSe_2$ NCs tend to become more irregular in shape with longer synthesis duration (comparing Figure 3(a-i) to (a-ii) (condition A), or (b-i) to (b-ii) (condition B)). Higher precursor concentration did not have significant effect toward the morphological uniformity. Because of weaker coordination of P3HT with the precursors, samples synthesized under condition C (see Figure 3(c-i) and (c-ii)) are of larger size and wider size distribution. Of course, we cannot completely rule out the possibility of agglomeration when the weaker polymeric ligand P3HT is used. The lattice spacings in high-resolution TEM images are also consistent with that of $CuInSe_2$.

**3.4. Optical Absorption Properties of $CuInSe_2$ Nanocrystals.** Figure 4 shows the absorption spectra of $CuInSe_2$ NCs, whereas the spectrum of P3HT is also given for comparison. The absorbance tails in the near IR range can be observed from all spectra of the $CuInSe_2$ NCs, i.e., samples A, B, and C (30 min), confirming the formation of the ternary chalcogenide nanocrystals. Sample C also retains an absorption peak at about 450 nm, which is attributed to the presence of P3HT after purification, although there is no obvious difference for spectra of sample A and sample B. It is perhaps useful to mention that because the Bohr radius of $CuInSe_2$ is 10.6 nm,[38] shift of absorbance edge with size change or the quantum confinement effect was not observed because all of our NCs are either larger than or comparable to the Bohr radius.

For comparison, the spectrum of NCs prepared at 250 °C is given as the inset in Figure 4 which shows the presence of a broad but noticeable absorption peak at ~1100 nm. This absorption peak is believed to be due to $Cu_{2-x}Se$ species according to an earlier study on binary system.[39] On the other hand, the ternary $CuInSe_2$ is not expected to have any absorption peak in this region. It is worth mentioning that $Cu_{2-x}Se$ is very easily detected by absorption spectroscopy because of its high absorption coefficient, which is 2 or 3 orders of magnitude higher than that of $CuInSe_2$ ($1 \times 10^7$ $cm^{-1}$ for $Cu_{2-x}Se$ and $1 \times 10^4$ to $1 \times 10^5$ $cm^{-1}$ for $CuInSe_2$).[40] Our initial selection of synthesis conditions was carried out by monitoring the absorption peak of $Cu_{2-x}Se$. Therefore, the absence of absorption at ~1100 nm in the absorption spectra of

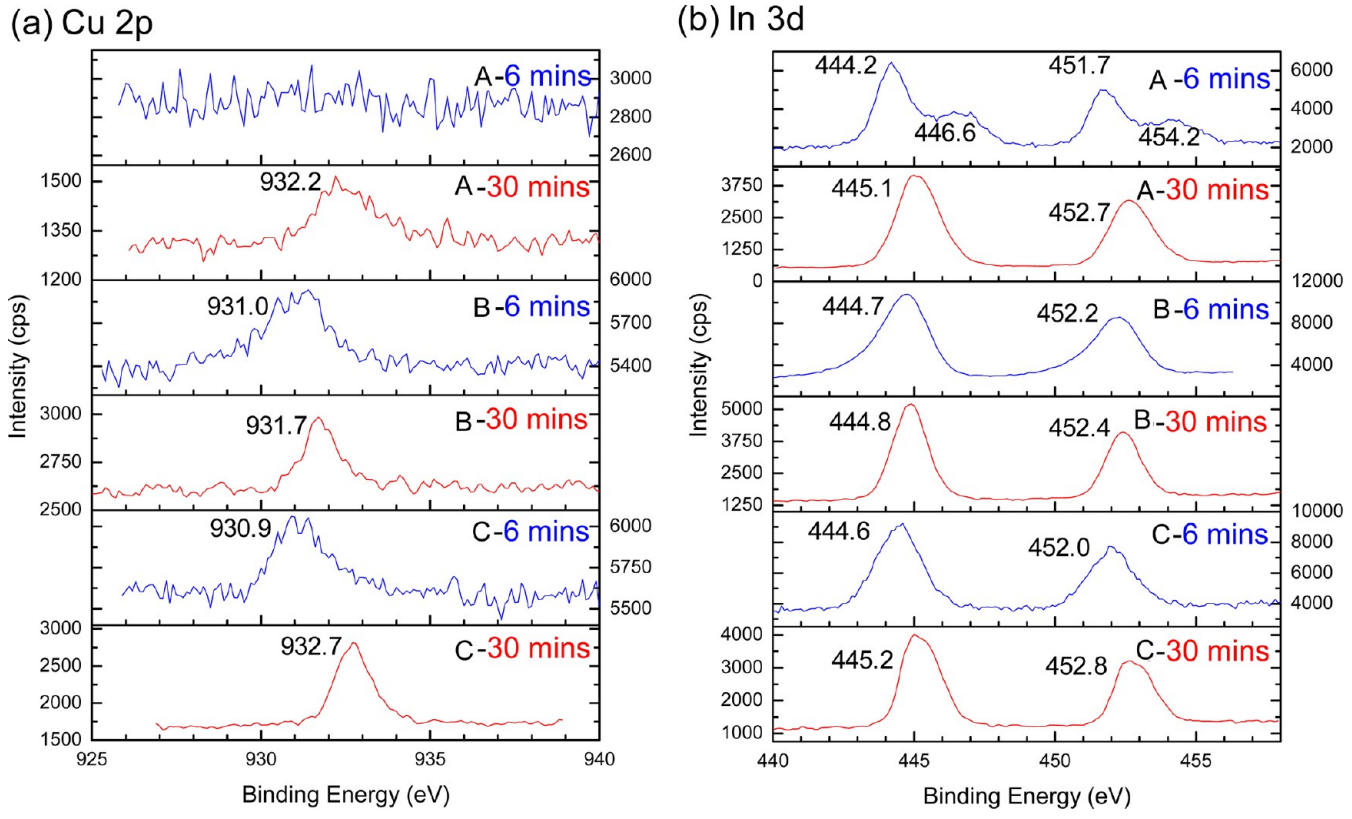


**Figure 2.** Individually (a) Cu2p and (b) In3d core level BE spectra of the $CuInSe_2$ NCs. The theoretical Cu2p and $In3d_{5/2}$ BE positions of $CuInSe_2$ are 931.9 and 444.7 eV.[37]

our samples prepared under condition A, B, and C at 290 °C/260 °C (injection/growth temperature) indicates that the reaction of binary $Cu_{2-x}Se$ species toward $CuInSe_2$ is rather complete. Although the analysis of absorption properties does not provide quantitative information on detailed stoichiometry, it complements other analytical techniques.

## 4. DISCUSSION

**4.1. Formation Mechanism of Core−Shell-like $CuInSe_2$ Nanocrystals.** Single-step synthesis of chalcogenide NCs or nanorods with inhomogeneous stoichiometry had been previously demonstrated;[41−44] the results were attributed to the differences in (i) precursor reactivities and (ii) affinities of coordination species toward precursors. These studies usually focus on the anionic species (e.g., $Se^{2-}$ and $S^{2-}$) or do not involve n- and p-type transition. Previous studies on $CuInSe_2$ and $CuInS_2$ formation suggested sequential formation of Cu-rich nuclei and In incorporation.[24,45,46] Our results clearly indicate that the formation of the Cu-based monomers is more favorable. Different monomer formation kinetics of $Cu(acac)_2$ and $In(acac)_3$ are believed to be responsible for the gradient stoichiometry. The kinetics is dependent on the specific coordination between the nucleophilic TOP-Se and metallic species precursors. This can be understood based on the "degree of supersaturation" (DS) of Cu-based or In-based monomers. Upon injection of TOP-Se, the DS of [CuSe] monomer is higher as compared to that of [InSe] due to preferential binding between Cu and TOP-Se. The required size of stable embryonic nucleus is smaller at higher DS. To further understand this point, we carried out hot-injection synthesis using only individually $Cu(acac)_2$ or $In(acac)_3$ under the same conditions. The TEM images of the $Cu_{2-x}Se$ and $In_2Se_3$ binary NCs (see Figure S1 in the Supporting Information) show that the $Cu_{2-x}Se$ is much larger than $In_2Se_3$. Their size distribution is also included in Figure S2 in the Supporting Information. The results support our hypothesis that $Cu_{2-x}Se$ formed at a much fast rate that $In_2Se_3$.

Interestingly, our proposed favorable formation of Cu-based monomer contradicts the facts that (i) the theoretical cleavage energy of ligated acetylacetonate groups from $Cu(acac)_2$ is high than that of $In(acac)_3$,[47] and (ii) our thermogravimetric analysis results showing $Cu(acac)_2$ decomposes at higher temperature than $In(acac)_3$ (see Figure S3 in the Supporting Information). These contradictions highlight the critical influence of specific coordination between nucleophilic ligands and precursors. Based on 'hard soft acid base' (HSAB) principle, the phosphine group in TOP-Se, a soft base, prefers coordination with soft acid $Cu^{2+}$ or $Cu^{1+}$, rather than with the hard acid $In^{3+}$. Such preferential coordination is expected to have enhanced the Cu precursor reactivity. In fact, the concept of intermediate binding state before monomer formation was proposed by several researchers in their studies of binary systems such as ZnSe.[36] The usage of P3HT substantially reduced the reactivity difference by interfering with the precursor binding process which might affect both the monomer formation and reactivity. P3HT reduced the stoichiometry gradient substantially although it is unable to completely eliminate this difference in reactivity that resulted in $CuInSe_2$ NCs with core−shell-like stoichiometry.

**4.2. Role of P3HT.** P3HT as a weaker coordination species (competing with TOP) has the functions of (i) moderating the gradient stoichiometry and (ii) enhancing interfacial charge transport. Previous work on CdS suggested that sulfur in the thiophene ring of P3HT could coordinate with $Cd^{2+}$.[7] It is

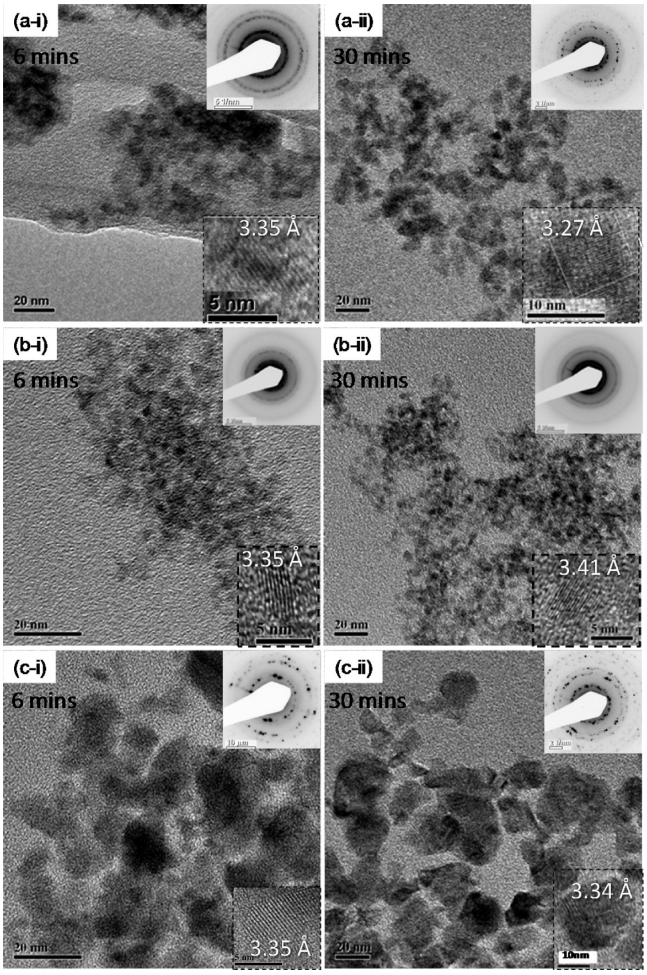


**Figure 3.** Morphologies of $CuInSe_2$ NCs synthesized with 6 and 30 min reaction time. (a-i, a-ii) Samples prepared under condition A, (b-i, b-ii) samples prepared under condition B, and (c-i, c-ii) samples prepared under condition C.

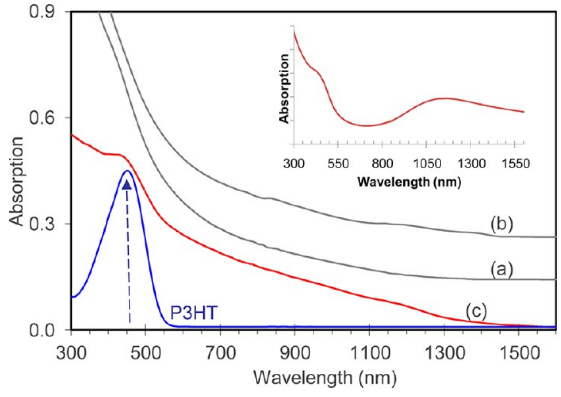


**Figure 4.** Absorption spectra of the $CuInSe_2$ NCs obtained after 30 min synthesis duration. (a) Sample prepared under condition A-30 min, (b) sample prepared under condition B-30 min, and (c) sample prepared under condition C-30 min as compared to that of pure P3HT. Spectra were vertically shifted for better clarify. The spectrum (see inset) of a sample prepared at a lower injection and growth temperature 250 °C shows a broad absorption peak at IR region which is characteristic of $Cu_{2-x}Se$ species.

believed that coordination between S and $Cu^{2+}$ (or $Cu^{1+}$) also existed in our system. The moderation of the gradient stoichiometry due to P3HT can be again explained using the HSAB principle. S as a soft Lewis base preferentially coordinates with soft acid $Cu^{2+}$ or $Cu^{1+}$ rather than with hard acid $In^{3+}$. Therefore, P3HT competes with TOP-Se in binding with Cu and this leads to moderation of reactivity difference between Cu and In precursors. Other important considerations include the more rigid polymeric structure and larger steric effect of P3HT (as compared with those of TOP) that may alter physical environment of crystal growth.

The conducting polymer–NC hybrids were demonstrated to have high potential for applications including photovoltaic, optoelectronic, and transistor devices. In this study, P3HT–$CuInSe_2$ NC hybrid is anticipated to be potentially a highly sensitive photodetector, due to core–shell-like structure and desirable enhanced NCs-polymer interfacial charge transfer. The preliminary photoconductivity data revealed that the photocurrent of P3HT–$CuInSe_2$ NCs (i.e., $CuInSe_2$ prepared in the presence of P3HT) is much more sensitive to light irradiation in comparison to $CuInSe_2$ NCs synthesized without the presence of P3HT (see Figure S4 in the Supporting Informatiom). The much higher photosensitivity of P3HT–$CuInSe_2$ NCs is believed to be contributed by direct capping of P3HT onto $CuInSe_2$ NCs that facilitates charge separation and transport upon irradiation. It is important to mention that no ligand exchange was carried out for preparation of photoconductivity sample. It is also believed that the actual mechanisms are more complex and further studies on effects of P3HT and the gradient stoichiometry toward photoconductivity are planned.

## 5. CONCLUSIONS

We report here a hot-injection synthesis of P3HT–$CuInSe_2$ NC hybrid, in which the NCs possess a radially increasing $In^{3+}$:$Cu^{1+}$ atomic ratio. This core–shell-like structure is a result of different reactivities of metallic species precursors during monomer formation and subsequent nucleation and crystal growth. Formation of Cu or In-based monomers is affected by dissimilar coordination affinity between the Cu or In precursors with functional group of nucleophilic ligands, e.g., phospine in TOP-Se. The presence of P3HT during NC synthesis moderated the reactivity difference between the two metallic species precursors, resulting in tuning of gradient stoichiometry. Such conducting polymer–NC hybrids facilitated interfacial carrier separation and transport, and can be readily incorporated into device architecture without any ligand exchange. The underlying principle drawn from this work also suggests the feasibility of manipulating semiconducting properties of various chalcogenide NCs via stoichiometric tuning by intelligent selection of coordination species. The P3HT-$CuInSe_2$ NC hybrid with possibly tunable stoichiometry has shown potential for applications, e.g., in photodetectors.

## ■ ASSOCIATED CONTENT

### Supporting Information

(S1–S2) synthesis of individual Cu and In-based NCs (morphologies and size); (S3) thermogravimetric analysis results of $Cu(acac)_2$ and $In(acac)_3$; (S4) demonstration of photodetector application of P3HT-$CuInSe_2$ NC hybrid. This material is available free of charge via the Internet at http://pubs.acs.org.

## AUTHOR INFORMATION


### Corresponding Author

*E-mail: asxhu@ntu.edu.sg. Fax: (65) 6790 9081. Tel: (65) 6790 4610.


### Author Contributions

The manuscript was written through contributions of all authors. Xiao Hu (PhD supervisor of Yen Nan Liang) oversaw the research work and wrote the paper together with Y.N.L. All authors have given approval to the final version of the manuscript.

### Notes

The authors declare no competing financial interest.

## ACKNOWLEDGMENTS

The authors acknowledge National Research Foundation (NRF) Singapore for support via a CRP program (CRP-2007-G-01). Y.N.L. thanks Dr. Yan Qingyu for discussion on synthesis design, Dr. Yu Kui for discussion on reaction mechanism, and Dr. Zhang Zheng (IMRE) on XPS analysis. The TFXRD, EDX, and TEM works were performed at the Facility for Analysis, Characterization, Testing and Simulation (FACTS) in Nanyang Technological University, Singapore.

## ABBREVIATIONS

$CuInSe_2$, copper indium selenide
P3HT, poly(3-hexyl thiophene)
NCs, nanocrystals
DBE, dibenzyl ether
$Cu(acac)_2$, copper acetylacetonate
$In(acac)_3$, indium acetylacetonate
TOP-Se, tri-n-octylphosphine selenide
TOP, tri-n-octylphosphine
TFXRD, thin film X-ray diffraction
AAS, atomic absorption spectroscopy
XPS, X-ray photoelectron spectroscopy
EDX, energy-dispersive X-ray spectroscopy
TEM, transmission electron microscopy
BE, binding energy
DS, degree of supersaturation
HSAB principle, "hard soft acid base" principle

## REFERENCES


(1) Zhao, L.; Lin, Z. *Adv. Mater.* **2012**, *24*, 4353−4368.
(2) Park, Y.; Advincula, R. C. *Chem. Mater.* **2011**, *23*, 4273−4294.
(3) Leventis, H. C.; King, S. P.; Sudlow, A.; Hill, M. S.; Molloy, K. C.; Haque, S. A. *Nano Lett.* **2010**, *10*, 1253−1258.
(4) Greenham, N. C.; Peng, X.; Alivisatos, A. P. *Phys. Rev. B* **1996**, *54*, 17628−17637.
(5) Graetzel, M.; Janssen, R. A. J.; Mitzi, D. B.; Sargent, E. H. *Nature* **2012**, *488*, 304−312.
(6) Dayal, S.; Kopidakis, N.; Olson, D. C.; Ginley, D. S.; Rumbles, G. *J. Am. Chem. Soc.* **2009**, *131*, 17726−17727.
(7) Liao, H.-C.; Chen, S.-Y.; Liu, D.-M. *Macromolecules* **2009**, *42*, 6558−6563.
(8) Stavrinadis, A.; Beal, R.; Smith, J. M.; Assender, H. E.; Watt, A. A. R. *Adv. Mater.* **2008**, *20*, 3105−3109.
(9) Watt, A. A. R.; Blake, D.; Warner, J. H.; Thomsen, E. A.; Tavenner, E. L.; Rubinsztein-Dunlop, H.; Meredith, P. *J. Phys. D: Appl. Phys.* **2005**, *38*, 2006−2012.
(10) Lee, Y.-H.; Chang, C.-J.; Kao, C.-J.; Dai, C.-A. *Langmuir* **2010**, *26*, 4196−4206.
(11) Warner, J. H.; Watt, A. A. R. *Mater. Lett.* **2006**, *60*, 2375−2378.
(12) Warner, J. H.; Watt, A. A. R.; Tilley, R. D. *Nanotechnology* **2005**, *16*, 2381−2384.
(13) Rockett, A.; Birkmire, R. W. *J. Appl. Phys.* **1991**, *70*, R81−R97.
(14) Chiang, M.-Y.; Chang, S.-H.; Chen, C.-Y.; Yuan, F.-W.; Tuan, H.-Y. *J. Phys. Chem. C* **2011**, *115*, 1592−1599.
(15) Jiang, Y.; Wu, Y.; Mo, X.; Yu, W.; Xie, Y.; Qian, Y. *Inorg. Chem.* **2000**, *39*, 2964−2965.
(16) Li, B.; Xie, Y.; Huang, J.; Qian, Y. *Adv. Mater.* **1999**, *11*, 1456−1459.
(17) Tang, J.; Hinds, S.; Kelley, S. O.; Sargent, E. H. *Chem. Mater.* **2008**, *20*, 6906−6910.
(18) Allen, P. M.; Bawendi, M. G. *J. Am. Chem. Soc.* **2008**, *130*, 9240−9241.
(19) Malik, M. A.; O'Brien, P.; Revaprasadu, N. *Adv. Mater.* **1999**, *11*, 1441−1444.
(20) Guo, Q.; Kim, S. J.; Kar, M.; Shafarman, W. N.; Birkmire, R. W.; Stach, E. A.; Agrawal, R.; Hillhouse, H. W. *Nano Lett.* **2008**, *8*, 2982−2987.
(21) Zhou, W.; Yin, Z.; Sim, D. H.; Zhang, H.; Ma, J.; Hng, H. H.; Yan, Q. *Nanotechnology* **2011**, *22*, 195607.
(22) Koo, B.; Patel, R. N.; Korgel, B. A. *J. Am. Chem. Soc.* **2009**, *131*, 3134−3135.
(23) Norako, M. E.; Brutchey, R. L. *Chem. Mater.* **2010**, *22*, 1613−1615.
(24) Wang, J.-J.; Wang, Y.-Q.; Cao, F.-F.; Guo, Y. -G.; Wan, L.-J. *J. Am. Chem. Soc.* **2010**, *132*, 12218−12221.
(25) Panthani, M. G.; Akhavan, V.; Goodfellow, B.; Schmidtke, J. P.; Dunn, L.; Dodabalapur, A.; Barbara, P. F.; Korgel, B. A. *J. Am. Chem. Soc.* **2008**, *130*, 16770−16777.
(26) Guo, Q.; Ford, G. M.; Hillhouse, H. W.; Agrawal, R. *Nano Lett.* **2009**, *9*, 3060−3065.
(27) de Kergommeaux, A.; Fiore, A.; Bruyant, N.; Chandezon, F.; Reiss, P.; Pron, A.; de Bettignies, R.; Faure-Vincent, J. *Sol. Energy Mater. Sol. Cells* **2011**, *95*, 39−43.
(28) Bereznev, S.; Kois, J.; Golovtsov, I.; Öpik, A.; Mellikov, E. *Thin Solid Films* **2006**, *511−512*, 425−429.
(29) Arici, E.; Hoppe, H.; Schäffler, F.; Meissner, D.; Malik, M. A.; Sariciftci, N. S. *Thin Solid Films* **2004**, *451−452*, 612−618.
(30) Arici, E.; Hoppe, H.; Schäffler, F.; Meissner, D.; Malik, M. A.; Sariciftci, N. S. *Appl. Phys. A: Mater. Sci. Process.* **2004**, *79*, 59−64.
(31) Yang, Y.; Zhong, H.; Bai, Z.; Zou, B.; Li, Y.; Scholes, G. D. *J. Phys. Chem. C* **2012**, *116*, 7280−7286.
(32) Guillén, C.; Herrero, J. *Thin Solid Films* **2001**, *387*, 57−59.
(33) Cojocaru-Miredin, O.; Choi, P.; Wuerz, R.; Raabe, D. *Appl. Phys. Lett.* **2011**, *98*, 103504−3.
(34) Steckel, J. S.; Yen, B. K. H.; Oertel, D. C.; Bawendi, M. G. *J. Am. Chem. Soc.* **2006**, *128*, 13032−13033.
(35) Liu, H.; Owen, J. S.; Alivisatos, A. P. *J. Am. Chem. Soc.* **2007**, *129*, 305−312.
(36) Yu, K.; Hrdina, A.; Zhang, X.; Ouyang, J.; Leek, D. M.; Wu, X.; Gong, M.; Wilkinson, D.; Li, C. *Chem. Commun.* **2011**, *47*, 8811−8813.
(37) Moulder, J. F.; Stickle, W. F.; Sobol, P. E.; Bomben, K. D., *Handbook of X-ray Photoelectron Spectroscopy*; Chastain, J., King, R. C. J., Ed.; Physical Electronics, Inc.: Eden Prairie, MN, 1995.
(38) Castro, S. L.; Bailey, S. G.; Raffaelle, R. P.; Banger, K. K.; Hepp, A. F. *Chem. Mater.* **2003**, *15*, 3142−3147.
(39) Deka, S.; Genovese, A.; Zhang, Y.; Miszta, K.; Bertoni, G.; Krahne, R.; Giannini, C.; Manna, L. *J. Am. Chem. Soc.* **2010**, *132*, 8912−8914.
(40) Hessel, C. M.; P. Pattani, V.; Rasch, M.; Panthani, M. G.; Koo, B.; Tunnell, J. W.; Korgel, B. A. *Nano Lett.* **2011**, *11*, 2560−2566.
(41) Bae, W. K.; Char, K.; Hur, H.; Lee, S. *Chem. Mater.* **2008**, *20*, 531−539.
(42) Li, L.; Reiss, P. *J. Am. Chem. Soc.* **2008**, *130*, 11588−11589.
(43) Yu, K.; Hrdina, A.; Ouyang, J.; Kingston, D.; Wu, X.; Leek, D. M.; Liu, X.; Li, C. *ACS Appl. Mater. Interfaces* **2012**, *4*, 4302−4311.
(44) Yu, K.; Ouyang, J.; Zhang, Y.; Tung, H.-T.; Lin, S.; Nagelkerke, R. A. L.; Kingston, D.; Wu, X.; Leek, D. M.; Wilkinson, D.; Li, C.; Chen, I.-G.; Tao, Y. *ACS Appl. Mater. Interfaces* **2011**, *3*, 1511−1520.

(45) Kruszynska, M.; Borchert, H.; Parisi, J. r.; Kolny-Olesiak, J. *J. Am. Chem. Soc.* **2010**, *132*, 15976−15986.
(46) Norako, M. E.; Franzman, M. A.; Brutchey, R. L. *Chem. Mater.* **2009**, *21*, 4299−4304.
(47) Stary, J.; Liljenzin, J. O. *Pure Appl. Chem.* **1982**, *54*, 2557−2592.